COMPARATIVE STUDY OF TURBO CODED WIDEBAND ADAPTIVE MODULATION AND SPACE-TIME TRELLIS CODES

T. H. Liew, B. L. Yeap and L. Hanzo

Dept. of ECS., Univ. of Southampton, SO17 1BJ, UK.
Tel: +44-703-593 125, Fax: +44-703-593 045
Email: thl,lh@ecs.soton.ac.uk, http://www-mobile.ecs.soton.ac.uk

ABSTRACT

Decision Feedback Equaliser (DFE) aided turbo coded wideband Adaptive Quadrature Amplitude Modulation (AQAM) is capable of accommodating the temporal channel quality variation of fading channels. By contrast, the family of multiple-input-multiple-output (MIMO) DFE aided space-time trellis codes benefits from transmit diversity and hence it is capable reducing, rather than accommodating the temporal channel quality fluctuations. The performance of both systems is characterised and compared when communicating over the COST 207 Typical Urban (TU) wideband fading channel. It was found that the turbo coded AQAM scheme outperforms the two-transmitter Space-Time Trellis Coded (STTC) system employing two receivers, although its performance becomes inferior to that of a STTC arrangement employing more than two receivers.

1. INTRODUCTION

Adaptive Quadrature Amplitude Modulation (AQAM) [1,2] employs a higher-order modulation scheme, when the channel quality is favourable, in order to increase the number of Bits Per Symbol (BPS) transmitted and conversely, a more robust lower-order modulation scheme is activated, when the channel exhibits a reduced instantaneous quality, for the sake of improving the mean Bit Error Ratio (BER) performance. When applying AQAM for transmission over wideband channels, the decision feedback equaliser (DFE) employed will eliminate most of the Inter Symbol Interference (ISI). Consequently, the associated pseudo-Signal to Noise Ratio (SNR) at the output of the DFE, which will be defined in the context of Equation 1, is calculated and used as a metric for activating the appropriate modulation modes. This ensures that the performance is optimised by employing channel equalised AQAM, in order to jointly combat the signal power Co-Channel Interference (CCI) and ISI fluctuations experienced in a wideband channel. Furthermore, the error correction and error detection capability of various channel coding schemes [3] can be exploited for improving the BER and BPS throughput performance of wideband AQAM [6–8].

The third generation (3G) mobile communication standards [4] are expected to offer a wide range of bearer services, spanning from voice to high-rate data services supporting rates of at least 144 kb/s in vehicular, 384 kb/s in outdoor-to-indoor and 2 Mb/s in indoor as well as picocellular applications [9]. In an effort to support such high rates, the capacity of band-limited wireless channels can be increased by employing multiple transmit antennas. Recently, different transmit diversity techniques have been introduced, in order to provide diversity gain for MSs by upgrading the BSs. In [5], Tarokh *et al.* proposed space-time trellis coding by jointly designing the channel coding, modulation, transmit diversity and the optional receiver diversity [3].

In this contribution, the Multiple Input Multiple Output (MIMO) equaliser [10,11] was employed in conjunction with space-time trellis codes for equalising the wideband channel. The Minimum Mean Squared Error (MMSE) MIMO equaliser was first studied by Duel-Hallen [10] in the transform domain. It was then employed by Tidestav *et al.* in [11] for multiuser detection. In Space-Time Trellis Codecs (STTC) [3, 5] there are multiple transmitters and receivers at both the transmitting and receiving ends. The received symbol at each receiver is constituted by the superposition of all transmitted symbols, which undergo independent wideband fading. The MIMO equaliser is employed for equalising and estimating the transmitted symbols of each transmitter. In [12], we have shown that as we increase the diversity order of STT coding, the time-variant fluctuation of the channel quality becomes less severe, since with the advent of diversity the fading channels have been converted to AWGN-like channels. By contrast, AQAM seeks to accommodate the temporal variation of the quality of fading channels by appropriately adjusting the turbo coded AQAM modes. Therefore in this contribution, we will investigate the achievable throughput of turbo coded AQAM and space-time trellis codes.

2. SYSTEM OVERVIEW

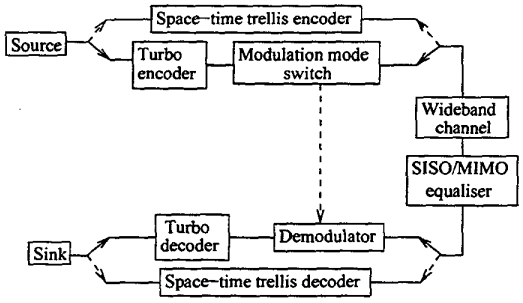

Figure 1: System overview of the turbo coded AQAM and space-time trellis schemes.

The financial support of the EPSRC, UK and that of the European Union is gratefully acknowledged.

0-7803-7484-3/02/$17.00 ©2002 IEEE.

Figure 1 shows the system overview of the proposed turbo coded AQAM scheme as well as the space-time trellis codes employed. At the transmitter, the information source generates random information data bits. In our proposed turbo coded AQAM scheme, the information data bits are encoded by the turbo convolutional encoder. Assuming that the next transmission burst's short term channel quality can be estimated as in a Time Division Duplexing (TDD) scheme, a suitable AQAM mode will be chosen by the modulation mode switch shown in Figure 1. The turbo coded bits are subsequently mapped to the AQAM symbols. By contrast, the information bits will be directly encoded by the STT encoder, which produces the modulated symbols depending on the specific STT code employed. The modulated symbols are transmitted over the COST 207 TU wideband channel [13]. At the receiver, the received symbols are equalised by the appropriate Single Input Single Output (SISO) or MIMO DFE, respectively. Depending on the specific AQAM mode chosen at the transmitter, the demodulator provides soft outputs for the turbo decoder based on the equalised symbols output by the SISO equaliser. The turbo decoded bits are passed to the information sink for the calculation of the BER, as shown in Figure 1. By contrast, the equalised symbols output by the MIMO equaliser are passed to the space-time trellis decoder.

2.1. SISO Equaliser and AQAM

At the receiver, the channel impulse response (CIR) is estimated, which is then used for calculating the SISO DFE coefficients [14]. Subsequently, the DFE is used for equalising the ISI-corrupted received signal. Additionally, both the channel quality estimate and the SISO DFE coefficients are utilised for computing the pseudo-SNR at the output of the SISO DFE. More explicitly, by assuming that the residual ISI is Gaussian distributed and that the probability of decision feedback errors is negligible, the pseudo-SNR at the output of the SISO DFE, γ, can be calculated as [15]:

$$\gamma = \frac{\text{Wanted Signal Power}}{\text{Residual ISI Power} + \text{Effective Noise Power}}. \quad (1)$$

This pseudo-SNR γ is then compared against a set of AQAM switching threshold levels, and subsequently the appropriate modulation mode is selected for the next transmission burst, assuming the availability of a reliable, low-delay feedback message, which can be transmitted to the remote receiver by superimposing it - after strongly protecting it - on the reverse-direction information [2]. However, in this treatise we will assume perfect AQAM mode signalling. The AQAM modes that are utilised in this system are Binary Phase Shift Keying (BPSK), Quadrature Phase Shift Keying (QPSK), 16-level Quadrature Amplitude Modulation (16QAM), 64-level Quadrature Amplitude Modulation (64QAM) and a 'No Transmission' (NO TX) mode.

2.2. MIMO Equaliser

In the context of the MIMO equaliser, similarly to the AQAM receiver, the CIR is estimated and then used for calculating the MIMO DFE coefficients [11]. At the receiver Rx, the received signal is given by the superposition of all the transmitters' signals. For each channel delay m and each combination of the specific transmitters and receivers of the MIMO scheme, we have a specific CIR. Hence we can write the corresponding channel matrix as:

$$\mathbf{H}^m = \begin{pmatrix} h^m_{1,1} & h^m_{1,2} & \dots & h^m_{1,Tx} \\ \vdots & \vdots & \vdots\vdots & \vdots \\ h^m_{Rx,1} & h^m_{Rx,2} & \dots & h^m_{Rx,Tx} \end{pmatrix}, \quad (2)$$

where $h^m_{Rx,Tx}$ is the CIR of the transmission link from transmitter Tx to receiver Rx at a channel delay of m. Consequently, we can write the channel matrix of the MIMO wideband channel as:

$$\mathbf{H} = (\mathbf{H}^0, \mathbf{H}^1, ..., \mathbf{H}^{N_c}), \quad (3)$$

where N_c is the maximum delay of the wideband channel.

The minimum mean squared error MIMO DFE feed-forward filter matrix is given by solving the following system of equations for $\mathbf{S}$ [11]:

$$(\mathbf{F}\mathbf{F}^H + \Psi) \cdot \begin{pmatrix} \mathbf{S}_0^H \\ \mathbf{S}_1^H \\ \vdots \\ \mathbf{S}_{N_f}^H \end{pmatrix} = \begin{pmatrix} \mathbf{H}_{N_f} \\ \mathbf{H}_{N_f-1} \\ \vdots \\ \mathbf{H}_0 \end{pmatrix}, \quad (4)$$

where $\mathbf{S}^H$ denotes the Hermitian transpose of $\mathbf{S}$ and N_f is the forward filter length, $\mathbf{F}$ is defined by

$$\mathbf{F} = \begin{pmatrix} \mathbf{H}^0 & \mathbf{H}^1 & \mathbf{H}^2 & \dots & \mathbf{H}^{N_f-1} \\ \mathbf{0} & \mathbf{H}^0 & \mathbf{H}^1 & \dots & \mathbf{H}^{N_f-2} \\ \vdots & \vdots & \vdots & \vdots\vdots & \vdots \\ \mathbf{0} & \mathbf{0} & \mathbf{0} & \dots & \mathbf{0} \end{pmatrix}, \quad (5)$$

and $\Psi = \mathbf{I} \cdot N_0$ where $\mathbf{I}$ is identity matrix and N_0 is the noise spectral density.

After the feed-forward coefficients have been calculated using Equation 4, we can find the N_b backward coefficients with the aid of [11]:

$$Q_n = \sum_{m=\max(0,n-N_c+N_f-1)}^{\min(N_f,N_f+n+1)} \mathbf{S}_m \cdot \mathbf{H}_{N_f+1-m+n}. \quad (6)$$

3. SIMULATION PARAMETERS

The space-time trellis codes employed in this treatise were proposed by Tarokh *et al.* in [5]. We chose 4PSK, 8PSK and 16PSK space-time trellis codes, which provide a throughput of 2, 3 and 4 BPS, respectively. All space-time trellis codes employ 16 states and the Viterbi Algorithm (VA) was used for their decoding.

Code	Octal generator polynomial	No. of states	Decoding algorithm	No. of iterations
TC(2,1,3)	7,5	4	Log-Map	8

Table 1: Parameters of the TC(2,1,3) code.

In this treatise, we employed Turbo Convolutional (TC) codes [3] employing constraint length 3 convolutional codes as their component codes. The associated parameters are shown in Table 1. Puncturing was applied to the TC codes for achieving different coding rates. We show in Table 2 the puncturing patterns employed and the resultant coding rates. The puncturing patterns seen in the table consist of two parts. Specifically, the associated different puncturing patterns represent the puncturing patterns of the parity bits emanating from the first and second decoder, respectively. Note that the puncturing patterns employed in these systems have been determined experimentally, but they are not claimed to be optimal. For procedures on designing high-rate turbo codes with the aid of puncturing the interested reader is referred to [16]. Different modulation

schemes were employed, which consequently result in different effective BPS throughputs, as shown in Table 2. The random turbo interleaver and random channel interleaver depths were chosen such that each AQAM transmission burst can be individually decoded, i.e. burst-by-burst turbo decoding was used. Additionally, in an effort to quantify the best possible performance of the system, we also studied a long-delay system, where the channel interleaver depth was chosen to be approximately 10^5 bits in the context of all AQAM modes. The associated channel interleaver depth and the corresponding turbo interleaver depth is indicated by the 'Long delay' phrase in Table 2.

Code Rate R	Puncturing Pattern	Modulation Mode	BPS	Random turbo interleaver depth	Random channel interleaver depth
0.33	1, 1	BPSK	0.33	228	684
		QPSK	0.66	456	1368
		Long delay		34198	102600
0.50	10, 01	BPSK	0.50	342	684
		QPSK	1.00	684	1368
		16QAM	2.00	1368	2736
		Long delay		51300	102600
0.75	100000 001000, 001000 000010	BPSK	0.75	513	684
		QPSK	1.50	1026	1368
		16QAM	3.00	2052	2736
		64QAM	4.50	3078	4104
		Long delay		76950	102600
0.83	10000 00000, 00000 00001	BPSK	0.83	570	684
		QPSK	1.66	1140	1368
		16QAM	3.32	2280	2736
		64QAM	4.98	3420	4104
		Long delay		85500	102600
0.90	04000 0020_{16}, 80000 1000_{16}	BPSK	0.90	615	684
		QPSK	1.80	1230	1368
		16QAM	3.60	2462	2736
		64QAM	5.40	3694	4104
		Long delay		92340	102600

Table 2: Simulation parameters associated with the TC channel codec in Figure 1.

Our studies were conducted for transmission over the COST 207 Typical Urban (TU) [13] channel. The corresponding CIR $h(t)$ is characterised as follows:

$$h(t) = 0.8507 \cdot \delta(t) + 0.3942 \cdot \delta(t - 4T) + 0.2683 \cdot \delta(t - 6T) + 0.2214 \cdot \delta(t - 7T). \quad (7)$$

Each path was faded independently according to the Rayleigh distribution and the corresponding normalised Doppler frequency was 3.27×10^{-5}. Both the SISO and the MIMO DFE incorporated 35 feed forward taps and 7 feedback taps and the transmission burst structure used in our treatise is shown in Figure 2. The following assumptions were stipulated. Firstly, the CIR was time-invariant for the duration of a transmission burst, but varied from burst to burst, which corresponds to assuming that the CIR is slowly varying. Secondly, perfect channel estimation and perfect knowledge of the AQAM mode used was assumed at the receiver. In practice a simple repetition code can be used for conveying the AQAM mode to the receiver. Furthermore, the modulation mode can also be detected blindly [1]. Thirdly, the pseudo-SNR at the output of the equaliser is estimated perfectly prior to transmission, which again, tacitly assumes the existence of a reliable, low-delay feedback path between the transmitter and the receiver. In practice, there will be error propagation in the DFE's feedback loop, which will degrade the performance of the system.

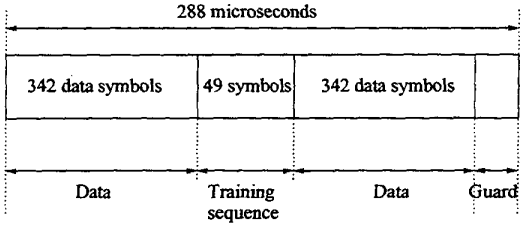

Figure 2: Transmission burst structure of the non-spread data.

4. SIMULATION RESULTS

4.1. Wideband STTC Performance

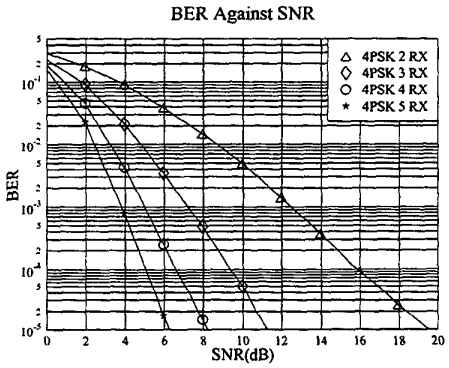

Figure 3: BER performance comparison between various 16-state 4PSK space-time trellis codes [5] using 2, 3, 4 and 5 receivers for transmission over the Rayleigh fading COST207 TU channel of Equation 8.

In Figure 3, we show the BER performance of a range of 16-state 4PSK space-time trellis codes using 2 to 5 receivers [5]. At a BER of 10^{-4}, we observe that there is a huge SNR improvement of more than 15 dB, when the number of receivers is increased from two to three. As the number of receivers is further increased to four and five, the incremental performance gain becomes smaller and smaller. Similar trends can be observed also for 16-state 8PSK and 16PSK space-time trellis codes although these results were omitted here due to lack of space.

4.2. Wideband STTC and AQAM Performance

In the previous section, we presented wideband performance results for the space-time trellis codes employed in conjunction with a MIMO equaliser. Let us now study the required SNR of the space-time trellis codes comparatively in terms of their achievable BPS throughput, when aiming for a target BER of 10^{-4}. These results will then be compared to the BPS performance of the uncoded AQAM schemes [2] at a BER of 10^{-4} in Figure 4.

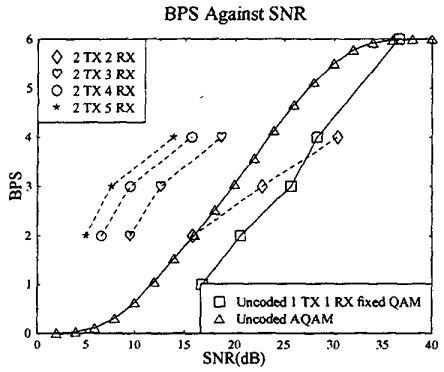

Figure 4: BPS performance comparison between space-time trellis codes [5], uncoded AQAM and the uncoded fixed modulation modes, when communicating over the Rayleigh fading COST207 TU channel of Equation 8. The target BER is 10^{-4}.

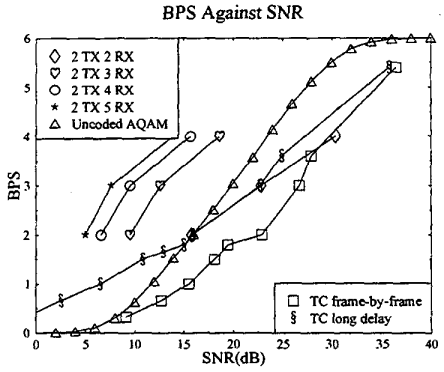

Figure 5: BPS performance comparison between space-time trellis codes [5], uncoded AQAM and TC codes in conjunction with both burst-by-burst decoding and long delay channel interleaving for transmission over the Rayleigh fading COST207 TU channel of Equation 8. The associated coding parameters are shown in Tables 1, 2 and the target BER is 10^{-4}.

Explicitly, there are two sets of curves in Figure 4. The curves drawn in continuous line represent the system having no diversity gain i.e. that employing one transmitter and one receiver. By contrast, the curves drawn using broken line represent the system having diversity gain due to employing space-time trellis codes and multiple receivers. The curve marked with squares represents the performance of the uncoded system using 1, 2, 3, 4 and 6 BPS fixed modulation schemes. In [1,2], an uncoded wideband burst-by-burst adaptive modem was characterised and its performance was reproduced in Figure 4, which is denoted by the triangles. We can see in Figure 4 that by employing space-time trellis codes in conjunction with two receivers, we have an SNR gain of 5 dB at a throughput of 2 BPS as compared to the uncoded system. The achievable SNR performance gain reduces to 3 dB, when the required throughput of the system is increased to 3 BPS and there is a negative SNR gain, when the required system throughput is 4 BPS. When employing AQAM, the single-transmitter and single-receiver system outperforms the space-time trellis code using two receivers. By contrast, the AQAM BPS performance remains inferior to that of the space-time trellis code using three or more receivers, as shown in Figure 4.

4.3. Wideband STTC, AQAM and Turbo Coded Fixed-Mode QAM Performance

In Figure 4, we have portrayed the performance of the $1-6$ BPS uncoded one-transmitter and one-receiver based fixed-mode modulation schemes, which was outperformed by the burst-by-burst AQAM scheme proposed in [1,2]. We will now investigate the required SNR of the turbo coded fixed modulation scheme in terms of the achievable BPS throughput, when aiming for a target BER of 10^{-4}. In Figure 5 we show the BPS performance of the TC(2,1,3) code [3] for both the short and long channel interleaver aided scenarios[1]. Recall that the length of the short channel interleaver was chosen such that it enabled burst-by-burst turbo decoding, while the long channel interleaver depth was approximately 10^5 bits. It can be seen that burst-by-burst turbo decoding in conjunction with the fixed-mode modulation schemes is inferior to the uncoded AQAM scheme. If, however, the delay permitted by the system allows the employment of a channel interleaver length of approximately 10^5 bits, we can clearly see in Figure 5 that there is a substantial SNR improvement over the burst-by-burst decoded scenario using the same fixed-mode modulation schemes. For the TC(2,1,3) code we can observe that the system outperforms uncoded AQAM for throughput values below 2 BPS. At 0.5 BPS, we can see in Figure 5 that the TC(2,1,3) code outperforms the uncoded AQAM scheme in required SNR terms by approximately 10 dB.

[1]The associated curve indicates the maximum achievable BPS, which was generated by combining all the different throughput fixed mode modulation schemes with all the different coding rate schemes

4.4. Wideband STTC, AQAM as well as Turbo Coded Fixed-Mode and AQAM Performance

In Figure 5 we have investigated the performance of the TC(2,1,3) code in conjunction with fixed modulation based systems for both low and high channel interleaver lengths. Let us now fully exploit the error correction capability of turbo codes in the context of AQAM. In our earlier research we used a set of fixed AQAM mode switching thresholds, which was determined with the aid of Powell's or experimental optimisation [1,2,17]. However, the achievable throughput of the system can be further increased, when we optimise the AQAM switching thresholds for each individual channel SNR value using Lagrangian optimisation [1,18]. We note however that the solutions in [1,18] use no channel coding during the optimisation of the AQAM thresholds. Since employing Lagrangian optimisation might not be feasible for AQAM systems using turbo codes, a simple procedure was proposed in Section 11.4.3 of [3] for determining the switching thresholds and the highest-throughput coding rates for turbo coded AQAM systems at each average channel SNR value.

Let us hence apply the joint switching threshold and TC coding rate optimisation techniques proposed in Section 11.4.3 of [3] to the TC coded AQAM system. We will refer to this scheme in our future discourse as the Optimised Rate Turbo Coded (ORTC) AQAM arrangement. In Figure 6 the curve marked with diamonds represents the BPS performance of the ORTC AQAM scheme using burst-by-burst decoding. As we can see in the figure, the employment of ORTC AQAM substantially improves the performance of the system, when the channel SNR is low. For example, at 0.5

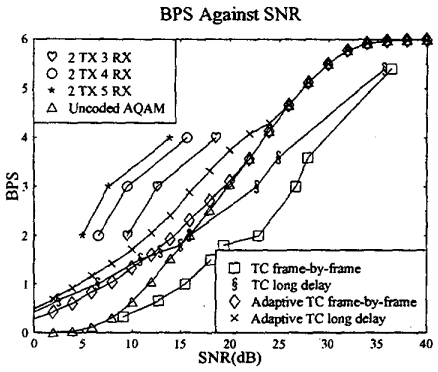

Figure 6: BPS performance comparison between space-time trellis codes [5], uncoded AQAM, ORTC AQAM using burst-by-burst decoding and long delay channel interleaver both with fixed and adaptive modulation, when communicating over the Rayleigh fading COST207 TU channel of Equation 8. The associated coding parameters are shown in Tables 1 and 2 and the target BER is 10^{-4}.

BPS we observe a 5 dB SNR gain over the uncoded AQAM system. However, as the channel SNR is increased, the SNR gain due to TC coding is reduced and uncoded AQAM will be activated instead of ORTC AQAM for channel SNRs in excess of 20 dB. For channel SNRs below 13 dB we can observe in Figure 6 that the performance of the ORTC AQAM scheme is similar to that of the TC coded fixed modulation schemes using the long-delay 10^5-bit channel interleaver. Hence, with the aid of ORTC AQAM we can achieve as good a performance, as the long-delay optimised-rate TC coded fixed modulation scheme without incurring a long delay. More explicitly, with the aid of the AQAM system we were capable of reducing the interleaving delay without compromising the BPS throughput.

On the other hand, if a long delay is tolerable in the context of the ORTC AQAM system, the 10^5-bit channel interleaver can be employed in the system. The corresponding BPS performance is shown in Figure 6 by the curve marked with crosses. As we can see in the figure, there is a significant BPS performance improvement over the short-delay burst-by-burst decoded ORTC AQAM system. Observe also in Figure 6 that the system only switches to the uncoded AQAM scheme for channel SNRs in excess of 25 dB. The corresponding performance also approaches that of the space-time trellis codes using three receivers. At a throughput of 2 BPS we can observe that the long-delay AQAM scheme's SNR performance is about 2-3 dB inferior in comparison to that of the space-time trellis codes using three receivers.

5. CONCLUSION

In this contribution we comparatively studied the performance of space-time trellis codes and turbo coded AQAM schemes when communicating over the wideband COST 207 TU channel. It was found that the turbo coded AQAM scheme outperforms the two-transmitter space-time trellis coded system employing two receivers, although its performance is inferior to the space-time trellis coded arrangement employing three or more receivers. Turbo coded AQAM schemes can be viewed as a lower complexity alternative for mitigating the channel quality fluctuations of wideband wireless channels in comparison to multiple-transmitter and multiple-receiver based space-time codes. If the complexity of the latter schemes is affordable, the performance advantages of AQAM erode.

6. REFERENCES

[1] L. Hanzo, C. H. Wong and M. S. Yee, "Adaptive Wireless Transceivers", John Wiley-IEEE Press, 2002.

[2] C. H. Wong and L. Hanzo, "Upper-bound Performance of a Wideband Burst-by-Burst Adaptive Modem", *IEEE Transactions on Communications*, Vol. 48, March 2000, pp. 367-369.

[3] L. Hanzo, T. H. Liew and B. L. Yeap, "Turbo Coding, Turbo Equalisation and Space-Time Coding for Transmission over Fading Channels", John Wiley-IEEE Press 2002.

[4] J. S. Blogh and L. Hanzo, "Third-Generation Systems and Intelligent Wireless Networking", John Wiley-IEEE Press, 2002.

[5] V. Tarokh, N. Seshadri and A. R. Calderbank, "Space-Time Codes for High Data Rate Wireless Communication: Performance Criterion and Code Construction", *IEEE Transactions on Information Theory*, Vol. 44, no. 2 pp. 744-765, March 1998.

[6] T. Keller, T. Liew, and L. Hanzo, "Adaptive redundant residue number system coded multicarrier modulation," *IEEE Journal on Selected Areas in Communications*, vol. 18, pp. 2292–2301, November 2000.

[7] M. Yee, T. Liew, and L. Hanzo, "Burst-by-burst adaptive turbo coded radial basis function assisted feedback equalisation," *IEEE Transactions on Communications*, vol. 49, no. 11, pp. 1935-1945, November 2001.

[8] V. Lau and M. Macleod, "Variable-rate adaptive trellis coded QAM for flat-fading channels," *IEEE Transactions on Communications*, vol. 49, pp. 1550–1560, September 2001.

[9] P. Chaudhury, "The 3GPP Proposal for IMT-2000", *IEEE Communications Magazine*, Vol. 37, no. 12, pp. 72-81, December 1999.

[10] A. Duel-Hallen, "Equalizers for multiple input/multiple output channels and PAM systems with cyclostationary input sequence," *IEEE Journal on Selected Areas in Communications*, vol. 10, pp. 630–639, April 1992.

[11] C. Tidestav, M. Sternad and A. A. Ahlén, "Reuse Within a Cell - Interference Rejection or Multiuser Detection", *IEEE Transactions on Communications*, Vol. 47, October 1999, oo. 1511-1522.

[12] T. Liew and L. Hanzo, "Space-time block coded adaptive modulation aided OFDM," in *IEEE Globecom 2001*, (San Antonio, USA), pp. 136–140, 25-29 November 2001.

[13] Office for Official Publications of the European Communities, Luxembourg, *COST 207: Digital land mobile communications*, 1989.

[14] L. Hanzo, W. Webb, and T. Keller, eds., *Single- and Multi-carrier Quadrature Amplitude Modulation*. Wessex, England: John Wiley & Sons, Ltd, 3rd ed., 2000. ISBN 0471492396.

[15] J. Cheung and R. Steele, "Soft-decision feedback equalizer for continuous-phase modulated signals in wide-band mobile radio channels," *IEEE Transactions on Communications*, vol. 42, no. 2-4, pp. 1628-1638, 1994.

[16] O. Acikel and W. Ryan, "Punctured turbo-codes for BPSK/QPSK channels," *IEEE Transactions on Communications*, vol. 47, pp. 1315–1323, September 1999.

[17] J. M. Torrance and L. Hanzo, "On the Upper bound performance of adaptive QAM in a slow Rayleigh fading", *IEE Electronics Letters*, April 1996, pp. 169-171.

[18] B. Choi, T. Liew, and L. Hanzo, "Concatenated space-time block coded and turbo coded symbol-by-symbol adaptive OFDM and multi-carrier CDMA systems," in *Proceedings of IEEE VTC 2001 Spring*, (Rhodes, Greece), pp. 776–780, 6-9 May 2001.